Hindawi
Journal of Mathematics
Volume 2023, Article ID 7906656, 11 pages
https://doi.org/10.1155/2023/7906656

Research Article

Analysis of Numerical Method for Diffusion Equation with Time-Fractional Caputo–Fabrizio Derivative

Hanxiao Wang,[1] Xindong Zhang ,[1] Ziyang Luo,[1] and Juan Liu [2]

[1] *School of Mathematical Sciences, Xinjiang Normal University, Urumqi, Xinjiang 830017, China*
[2] *College of Big Data Statistics, Guizhou University of Finance and Economics, Guiyang 550025, China*

Correspondence should be addressed to Xindong Zhang; liaoyuan1126@163.com and Juan Liu; liujuan1999@126.com

Received 22 December 2022; Revised 27 February 2023; Accepted 21 March 2023; Published 3 May 2023

Academic Editor: Kolade M. Owolabi

In this paper, we propose a high-precision discrete scheme for the time-fractional diffusion equation (TFDE) with Caputo-Fabrizio type. First, a special discrete scheme of C-F derivative is used in time direction and a compact difference operator is used in space direction. Second, we discuss the convergence of the proposed method in discrete L^1-norm and L^2-norm. The convergence order of our discrete scheme is $O(\tau^2 + h^4)$, where τ and h are the temporal and spatial step sizes, respectively. The aim of this paper is to show that fractional operator without singular term is very useful for improving the accuracy of discrete scheme.

1. Introduction

Recently, fractional differential equations have been widely used in many fields, such as anomalous diffusion [1, 2], fluid mechanics [3], image processing [4], and so on. The nonlocality of fractional operators provides an explanation for the material with memory and hereditary in the real world. Fractional operators are suitable for describing all kinds of complex mechanical and physical behaviors. Fractional operator has a wide range of applications, but there are also some practical difficulties in solving corresponding fractional differential equation. It should be pointed out that only a few fractional differential equations can obtain their analytical solutions through complex functions, such as the Mittag-Leffler function [5], H-function [6], and Wright function [7]. Moreover, the calculation of the above special functions is also difficult. Therefore, it is very important to study the numerical solutions of fractional differential equations. Common numerical solution methods including finite element method [8], finite difference method [9, 10], meshless method [11, 12], and finite volume element [13].

In order to obtain higher precision numerical solutions, many authors have proposed and used compact difference scheme (CDS) for fractional problems. By using this scheme, the accuracy of spatial direction can be improved to the fourth order. CDS has been fully proved and applied. The following results are the relevant works we know: Ran and Zhang [14] introduced a new CDS to explore the fourth-order time-fractional subdiffusion equation. In [15], CDS was used to solve the fractional subdiffusion equation. In [16], Ye et al. proposed and analyzed CDS for the time distributed-order diffusion-wave equation on a bounded domain. The purpose of [17] was to present the CDS for the fourth-order fractional subdiffusion equation.

There are many definitions of fractional derivative, such as Caputo, Riemann-Liouville, and Grünwald-Letnikov, the results of them can be found in [18–25], among others. In 2015, based on the exponential kernel, Caputo and Fabrizio presented a new definition of fractional derivative [26], that is, Caputo-Fabrizio (C-F) fractional derivative. C-F fractional derivative is important and interesting to describe the behavior of some complex physical materials. Another interesting aspect is that it provides a new perspective for some areas of mechanical phenomena. Up to now, there are a lot of discussions on C-F fractional derivative. Losada and Nieto [27] introduced fractional integral based on C-F fractional derivative, and studied some related fractional differential equations. A second-order scheme of the space C-F fractional diffusion equation was obtained in [28]. In [29], Nieto used nonsingular kernel to solve fractional logistic differential equation and obtained an implicit solution. Atangana and Alqahtani [30] considered numerical solutions of space and time for the C-F fractional derivative associated with the groundwater pollution equation. In 2017, Mirza and Vieru [31] proposed the fundamental solutions to advection-diffusion equation with time-fractional C-F fractional derivative. The main aim of [32] was to consider the application of C-F fractional derivative to nonlinear Fisher's reaction-diffusion equation. Soori and Aminataei [33] studied two new approximations to C-F fractional equation on nonuniform meshes. Atangana et al. [34, 35] studied the numerical solution for fractional derivative without singular kernel. Some existence results of solutions to fractional differential equation based on fixed point theorems and C-F fractional derivative were discussed in [36]. Approximate solutions for two higher-order C-F fractional integro-differential equations were considered in [37]. Other interesting results about C-F fractional derivative can be found in [38–44], among others.

TFDE is obtained from the standard diffusion equation by replacing the first-order time derivative with a fractional derivative of order $\alpha\ (0<\alpha<1)$. TFDE was derived by considering continuous time random walk problems, which are in general non-Markovian processes. From a physical viewpoint, they are obtained from a fractional Fick law replacing the classical Fick law, which describes transport processes with a long memory [45]. Nigmatullin [46] pointed out that many of the universal electromagnetic, acoustic, and mechanical responses can be modeled accurately using fractional diffusion or diffusion-wave equations. In this paper, CDS is proposed to discrete the following TFDE:

$$\begin{cases} {}_{0}^{CF}D_t^{\alpha}u(x,t) = a\left(\dfrac{\partial^2 u}{\partial x^2}\right) + f(x,t), & x\in[0,L], t\in[0,T],\\ u(x,t)|_{t=0} = \varphi(x), & x\in[0,L],\\ u(0,t)=0, u(L,t)=0, & t\in[0,T], \end{cases} \tag{1}$$

where a represents the diffusion coefficient; this paper only discusses the case as a is a positive constant. $f(x,t)$ and $\varphi(x)$ are all given and sufficiently smooth functions. For $0<\alpha<1$, C-F fractional derivative is defined as

$$\begin{aligned} {}_{0}^{CF}D_t^{\alpha}u(t) &= \frac{1}{1-\alpha}\int_0^t u'(s)e^{-\frac{\alpha}{1-\alpha}(t-s)}\mathrm{d}s \\ &= \frac{1}{1-\alpha}\int_0^t u'(s)e^{-\sigma(t-s)}\mathrm{d}s, \sigma = \frac{\alpha}{1-\alpha}. \end{aligned} \tag{2}$$

In this paper, we use the property of the C-F fractional derivative to control the accuracy of the time direction for the TFDE and combine this property with the compact difference operator to achieve the overall accuracy to $O(\tau^2+h^4)$, which also expands the application of the C-F fractional derivative. This paper is outlined as follows: In Section 2, we describe some notations and lemmas to construct the discrete scheme of equation (1). In Section 3, we study the stability and convergence of the discrete scheme. In Section 4, two numerical experiments are considered to verify the efficiency and utility of the discrete scheme. Finally, Section 5 gives a brief conclusion.

2. The Numerical Scheme

In this section, we mainly consider the construction of discrete scheme for equation (1). Let us introduce some notations first. Let $x_j = jh$ with $j=0,1,\ldots,M$ and $t_n = n\tau$ with $n=0,1,\ldots,N$, where $h=L/M$ and $\tau = T/N$ and M and N are positive integers. Defining a grid function space $V_h = \{V | V = (V_0, V_1, \ldots, V_M)\}$. Let $u_j^n = u(x_j, t_n)$ and $f_j^n = f(x_j,t_n)$. For any function $U, V \in V_h$, the notations are as follows:

$$\begin{gathered} (U,V) = h\sum_{j=1}^{M-1} U_j V_j, \|U\| = \sqrt{(U,U)}, \\ \delta_x U_j = \frac{U_j - U_{j-1}}{h}, \delta_x^2 U_j = \frac{U_{j+1} - 2U_j + U_{j-1}}{h^2}, \\ j = 1,2,\ldots,M-1. \end{gathered} \tag{3}$$

We define a compact operator $\mathscr{H}$ as follows:

$$\mathscr{H}u_j^n = \begin{cases} \dfrac{1}{12}\left(u_{j-1}^n + 10u_j^n + u_{j+1}^n\right) = \left(1 + \dfrac{h^2}{12}\delta_x^2\right)u_j^n, & 1\le j\le M-1,\\ u_j^n, & j = 0, M. \end{cases} \tag{4}$$

Due to the arbitrariness of C, we allow the value of C to be different at different locations. We now introduce some lemmas that will be used in the construction of numerical scheme.

Lemma 1 (see [28]). *For any $t>0$, $u(t)$ is smooth enough. Let $0<\alpha<1$ with $\sigma = \alpha/(1-\alpha)$. Then,*

$${}_{0}^{CF}D_t^{\alpha}u_j^n = \frac{1}{1-\alpha}\sum_{k=1}^{n}\frac{u_j^k - u_j^{k-1}}{\sigma\tau}e^{-\sigma(n-k)\tau}\left(1 - e^{-\sigma\tau}\right) + O\left(\tau^2\right). \tag{5}$$

In Lemma 1, the main item on the right side of the equation can be calculated as follows, which will be used in the following discrete scheme:

$$\begin{aligned}
&\frac{1}{1-\alpha}\sum_{k=1}^{n}\frac{u_j^k-u_j^{k-1}}{\sigma\tau}e^{-\sigma(n-k)\tau}\left(1-e^{-\sigma\tau}\right)\\
&=\frac{1-e^{-\sigma\tau}}{(1-\alpha)\sigma\tau}\left(e^{-\sigma(n-1)\tau}\left(u_j^1-u_j^0\right)+\cdots+e^{-\sigma\tau}\left(u_j^{n-1}-u_j^{n-2}\right)+u_j^n-u_j^{n-1}\right)\\
&=\frac{1-e^{-\sigma\tau}}{(1-\alpha)\sigma\tau}\left(-e^{-\sigma(n-1)\tau}u_j^0-\left(1-e^{-\sigma\tau}\right)e^{-\sigma(n-2)\tau}u_j^1-\cdots-\left(1-e^{-\sigma\tau}\right)u_j^{n-1}+u_j^n\right)\\
&=\frac{1-e^{-\sigma\tau}}{(1-\alpha)\sigma\tau}\left(u_j^n-\sum_{k=1}^{n-1}\left(1-e^{-\sigma\tau}\right)e^{-\sigma(n-k-1)\tau}u_j^k-e^{-\sigma(n-1)\tau}u_j^0\right).
\end{aligned} \tag{6}$$

Lemma 2 (see [15]). *Suppose* $u(x)\in C^6[0,L]$, *then*

$$\mathscr{H}u_{xx}\left(x_j,t_n\right)=\delta_x^2u_j^n+O\left(h^4\right),1\le j\le M-1. \tag{7}$$

By Lemma 1, equation (1) can be written as

$$\begin{aligned}
&\frac{1}{1-\alpha}\sum_{k=1}^{n}\frac{u_j^k-u_j^{k-1}}{\sigma\tau}e^{-\sigma(n-k)\tau}\left(1-e^{-\sigma\tau}\right)\\
&=au_{xx}\left(x_j,t_n\right)+f_j^n+O\left(\tau^2\right),
\end{aligned} \tag{8}$$

i.e.,

$$\begin{aligned}
&\frac{1-e^{-\sigma\tau}}{(1-\alpha)\sigma\tau}\left(u_j^n-\sum_{k=1}^{n-1}\left(1-e^{-\sigma\tau}\right)e^{-\sigma(n-1-k)\tau}u_j^k\right)\\
&=au_{xx}\left(x_j,t_n\right)+f_j^n+\frac{1-e^{-\sigma\tau}}{(1-\alpha)\sigma\tau}e^{-\sigma(n-1)\tau}u_j^0+O\left(\tau^2\right).
\end{aligned} \tag{9}$$

Let $A_k=\left(1-e^{-\sigma\tau}\right)e^{-\sigma(n-1-k)\tau}, 1\le k\le n-1$, by equation (9), Lemma 2 and the definition of compact operator $\mathscr{H}$, we have

$$\begin{cases}
\mathscr{H}u_j^n-\dfrac{a}{\lambda}\delta_x^2u_j^n=\displaystyle\sum_{k=1}^{n-1}A_k\mathscr{H}u_j^k+e^{-\sigma(n-1)\tau}\mathscr{H}u_j^0+\frac{1}{\lambda}\mathscr{H}f_j^n+R_j^n,\\
u_j^0=\varphi\left(x_j\right),0\le j\le M,\\
u_0^n=u_M^n=0,1\le n\le N,
\end{cases} \tag{10}$$

where $\lambda=1-\left(e^{-\sigma\tau}/((1-\alpha)\sigma\tau\right)$ and $\|R_j^n\|\le C\left(\tau^2+h^4\right)$.

Let U_j^n represent the numerical approximation of $u\left(x_j,t_n\right)$. Omitting the small term R_j^n in equation (10), then we can get the following CDS for equation (1):

$$\begin{cases}
\mathscr{H}U_j^n-\dfrac{a}{\lambda}\delta_x^2U_j^n=\displaystyle\sum_{k=1}^{n-1}A_k\mathscr{H}U_j^k+e^{-\sigma(n-1)\tau}\mathscr{H}U_j^0+\frac{1}{\lambda}\mathscr{H}f_j^n,\\
U_j^0=\varphi\left(x_j\right),\ 0\le j\le M,\\
U_0^n=U_M^n=0,1\le n\le N.
\end{cases} \tag{11}$$

The fully discrete scheme equation (11) will be used in Section 4.

3. Stability Analysis and Error Estimates

In this section, we theoretically prove that the above numerical scheme is unconditionally stable and obtain the result of convergence for equation (11). For convenience, the subscript j can be omitted.

Lemma 3 (see [47]). *If* $V,W\in V_h$, *then* $\left(\delta_x^2V,W\right)=-\left(\delta_xV,\delta_xW\right)$.

Lemma 4 (see [28]). *Let* $0<\alpha<1$, $\sigma=\alpha/(1-\alpha)$, *we have*

$$0<\sum_{k=1}^{n-1}A_k<1. \tag{12}$$

Lemma 5 (see [17]). *For any grid function* $u\in V_h$, *then* $\|u\|^2\le\|\mathscr{H}u\|^2\le\|u\|^2$.

The following theorem is about stability of discrete scheme equation (11):

Theorem 1. *Let* $\mathrm{U^n}$ *be the numerical solution of equation (11). Then,*

$$\left\|U^n\right\|\le C\left(\left\|U^0\right\|+\max_{1\le s\le n}\left\|f^s\right\|\right),\quad 1\le n\le N, \tag{13}$$

where C *is a positive constant and* $U^0 = \varphi(x_j)$.

Proof. By equation (11), we can obtain

$$\mathcal{H}U^n - \frac{a}{\lambda}\delta_x^2 U^n = \sum_{k=1}^{n-1} A_k \mathcal{H}U^k + e^{-\sigma(n-1)\tau}\mathcal{H}U^0 + \frac{1}{\lambda}\mathcal{H}f^n. \tag{14}$$

Multiplying both sides of equation (14) by $\mathcal{H}U^n$, we obtain that

$$\begin{aligned}&\left(\mathcal{H}U^n, \mathcal{H}U^n\right) - \frac{a}{\lambda}\left(\delta_x^2 U^n, \mathcal{H}U^n\right)\\ &= \left(\sum_{k=1}^{n-1} A_k \mathcal{H}U^k, \mathcal{H}U^n\right) + e^{-\sigma(n-1)\tau}\left(\mathcal{H}U^0, \mathcal{H}U^n\right)\\ &+ \frac{1}{\lambda}\left(\mathcal{H}f^n, \mathcal{H}U^n\right).\end{aligned} \tag{15}$$

From Lemma 3, we know

$$\begin{aligned}\left(\mathcal{H}U^n, \mathcal{H}U^n\right) \leq &\left(\sum_{k=1}^{n-1} A_k \mathcal{H}U^k, \mathcal{H}U^n\right)\\ &+ e^{-\sigma(n-1)\tau}\left(\mathcal{H}U^0, \mathcal{H}U^n\right) + \frac{1}{\lambda}\left(\mathcal{H}f^n, \mathcal{H}U^n\right).\end{aligned} \tag{16}$$

Next, we want to prove $\|\mathcal{H}U^n\| \leq C(\|\mathcal{H}U^0\| + \max_{1\leq s\leq n}\|\mathcal{H}f^s\|)$by mathematical induction, where $1 \leq n \leq N$. When $n = 1$, from equation (16), we obtain

$$\left(\mathcal{H}U^1, \mathcal{H}U^1\right) \leq \left(\mathcal{H}U^0, \mathcal{H}U^1\right) + \frac{1}{\lambda}\left(\mathcal{H}f^1, \mathcal{H}U^1\right). \tag{17}$$

According to Cauchy-Schwarz inequality, we obtain

$$\left\|\mathcal{H}U^1\right\|^2 \leq \left\|\mathcal{H}U^0\right\|\left\|\mathcal{H}U^1\right\| + \frac{1}{\lambda}\left\|\mathcal{H}f^1\right\|\left\|\mathcal{H}U^1\right\|, \tag{18}$$

i.e.,

$$\left\|\mathcal{H}U^1\right\| \leq \left\|\mathcal{H}U^0\right\| + \frac{1}{\lambda}\left\|\mathcal{H}f^1\right\| \leq C\left(\left\|\mathcal{H}U^0\right\| + \left\|\mathcal{H}f^1\right\|\right). \tag{19}$$

Assuming that

$$\left\|\mathcal{H}U^k\right\| \leq C\left(\left\|\mathcal{H}U^0\right\| + \max_{1\leq s\leq k}\left\|\mathcal{H}f^s\right\|\right). \tag{20}$$

holds for $k = 2, 3, \ldots, n-1$, we want to prove that

$$\left\|\mathcal{H}U^n\right\| \leq C\left(\left\|\mathcal{H}U^0\right\| + \max_{1\leq s\leq n}\left\|\mathcal{H}f^s\right\|\right). \tag{21}$$

For $k = n$, by equation (16) and Cauchy-Schwarz inequality, we know

$$\begin{aligned}\left\|\mathcal{H}U^n\right\|^2 \leq &\left\|\sum_{k=1}^{n-1} A_k \mathcal{H}U^k\right\|\left\|\mathcal{H}U^n\right\|\\ &+ e^{-\sigma(n-1)\tau}\left\|\mathcal{H}U^0\right\|\left\|\mathcal{H}U^n\right\| + \frac{1}{\lambda}\left\|\mathcal{H}f^n\right\|\left\|\mathcal{H}U^n\right\|,\end{aligned} \tag{22}$$

i.e.,

$$\left\|\mathcal{H}U^n\right\| \leq \sum_{k=1}^{n-1} A_k\left\|\mathcal{H}U^k\right\| + e^{-\sigma(n-1)\tau}\left\|\mathcal{H}U^0\right\| + \frac{1}{\lambda}\left\|\mathcal{H}f^n\right\|. \tag{23}$$

By equation (20), we have

$$\begin{aligned}\sum_{k=1}^{n-1} A_k\left\|\mathcal{H}U^k\right\| \leq\ & A_1C_1\left(\left\|\mathcal{H}U^0\right\| + |\mathcal{H}f^1\|\right) + A_2C_2\left(\left\|\mathcal{H}U^0\right\| + \max_{1\leq s\leq 2}\left\|\mathcal{H}f^s\right\|\right)\\ &+ \cdots + A_{n-1}C_{n-1}\left(\left\|\mathcal{H}U^0\right\| + \max_{1\leq s\leq n-1}\left\|\mathcal{H}f^s\right\|\right).\end{aligned} \tag{24}$$

Let $C = \max\{C_1, C_2, \ldots, C_{n-1}\}$. By Lemma 4, for the first term in right hand of equation (23), we arrive at

$$\begin{aligned}\sum_{k=1}^{n-1} A_k\left\|\mathcal{H}U^k\right\| &\leq (A_1 + A_2 + \cdots + A_{n-1})C\left(\left\|\mathcal{H}U^0\right\| + \max_{1\leq s\leq n-1}\left\|\mathcal{H}f^s\right\|\right)\\ &\leq C\left(\left\|\mathcal{H}U^0\right\| + \max_{1\leq s\leq n-1}\left\|\mathcal{H}f^s\right\|\right)\sum_{k=1}^{n-1} A_k.\end{aligned} \tag{25}$$

Using equation (20), we obtain

$$\begin{aligned}\|\mathscr{H}U^n\| &\le C\left(\|\mathscr{H}U^0\| + \max_{1\le s\le n-1}\|\mathscr{H}f^s\|\right)\\ &\quad + e^{-\sigma(n-1)\tau}\|\mathscr{H}U^0\| + \frac{1}{\lambda}\|\mathscr{H}f^n\| \\ &\le C\left(\|\mathscr{H}U^0\| + \max_{1\le s\le n}\|\mathscr{H}f^s\|\right).\end{aligned} \tag{26}$$

Therefore, it holds that $\|\mathscr{H}U^n\| \le C(\|\mathscr{H}U^0\| + \max_{1\le s\le n}\|\mathscr{H}f^s\|)$.

Applying Lemma 5, we obtain

$$\|U^n\| \le C\left(\|U^0\| + \max_{1\le s\le n}\|f^s\|\right), \tag{27}$$

where C is a positive constant. This completes the proof of the theorem.

Next, the convergence of discrete scheme equation (11) is analyzed. □

Theorem 2. *Let* u^{n} *be the exact solution of equation (1) and* U^{n} *be the numerical solution of equation (11). Let* $\varepsilon^{\mathrm{n}} = \mathrm{u}^{\mathrm{n}} - \mathrm{U}^{\mathrm{n}}$*, then* $\varepsilon^0 = 0$*. Then, it holds*

$$\|\varepsilon^n\| \le C\left(\tau^2 + h^4\right), 1 \le n \le N, \tag{28}$$

where C *is a positive constant.*

Proof. Subtracting equation (11) from equation (10), we obtain

$$\mathscr{H}\varepsilon^n - \frac{a}{\lambda}\delta_x^2\varepsilon^n = \sum_{k=1}^{n-1} A_k\mathscr{H}\varepsilon^k + e^{-\sigma(n-1)\tau}\mathscr{H}\varepsilon^0 + R^n. \tag{29}$$

Multiplying both sides of equation (29) by $\mathscr{H}\varepsilon^n$, we get that

$$\begin{aligned}\left(\mathscr{H}\varepsilon^n, \mathscr{H}\varepsilon^n\right) - \frac{a}{\lambda}\left(\delta_x^2\varepsilon^n, \mathscr{H}\varepsilon^n\right) &= \left(\sum_{k=1}^{n-1} A_k\mathscr{H}\varepsilon^k, \mathscr{H}\varepsilon^n\right)\\ &\quad + e^{-\sigma(n-1)\tau}\left(\mathscr{H}\varepsilon^0, \mathscr{H}\varepsilon^n\right) + \left(R^n, \mathscr{H}\varepsilon^n\right).\end{aligned} \tag{30}$$

According to Lemma 3 and Cauchy–Schwarz inequality, we know

$$\begin{aligned}\|\mathscr{H}U^n\|^2 &\le \left\|\sum_{k=1}^{n-1} A_k\mathscr{H}U^k\right\|\|\mathscr{H}U^n\| + e^{-\sigma(n-1)\tau}\|\mathscr{H}U^0\|\|\mathscr{H}U^n\|\\ &\quad + \frac{1}{\lambda}\|\mathscr{H}f^n\|\|\mathscr{H}U^n\|,\end{aligned} \tag{31}$$

i.e.,

$$\|\mathscr{H}\varepsilon^n\| \le \sum_{k=1}^{n-1} A_k\left\|\mathscr{H}\varepsilon^k\right\| + \|R^n\|. \tag{32}$$

Next, we want to prove $\|\mathscr{H}\varepsilon^n\| \le C(\tau^2 + h^4)$ by mathematical induction. For $n = 1$, by equation (32) and $\|R^n\| = \|R_j^n\| \le C(\tau^2 + h^4)$, we have

$$\|\mathscr{H}\varepsilon^1\| \le \|R^1\| \le C\left(\tau^2 + h^4\right). \tag{33}$$

Assuming that

$$\left\|\mathscr{H}\varepsilon^k\right\| \le C\left(\tau^2 + h^4\right), \tag{34}$$

holds for $k = 2, 3, \ldots, n-1$. Then, we want to show that equation (34) holds for $k = n$. By equation (34), for the first term in right hand of equation (32), we arrive at

$$\begin{aligned}\sum_{k=1}^{n-1} A_k\left\|\mathscr{H}\varepsilon^k\right\| &\le A_1C_1\left(\tau^2 + h^4\right) + A_2C_2\left(\tau^2 + h^4\right)\\ &\quad + \cdots + A_{n-1}C_{n-1}\left(\tau^2 + h^4\right).\end{aligned} \tag{35}$$

Let $C = \max\{C_1, C_2, \ldots, C_{n-1}\}$, by equations (32) and (34) and Lemma 4, we obtain

$$\begin{aligned}\|\mathscr{H}\varepsilon^n\| &\le C\left(\tau^2 + h^4\right)\sum_{k=1}^{n-1} A_k + \|R^n\|\\ &\le C\left(\tau^2 + h^4\right) + \|R^n\| \le C\left(\tau^2 + h^4\right).\end{aligned} \tag{36}$$

Therefore, it holds that $\|\mathscr{H}\varepsilon^n\| \le C(\tau^2 + h^4)$.

Applying Lemma 5, we arrive at $\|\varepsilon^n\|^2 \le \|\mathscr{H}\varepsilon^n\|^2 \le \|\varepsilon^n\|^2$ so that $\|\varepsilon^n\| \le \sqrt{3}\|\mathscr{H}\varepsilon^n\|$. Then,

$$\|\varepsilon^n\| \le C\left(\tau^2 + h^4\right), \tag{37}$$

where C is a positive constant. This completes the proof of the theorem. □

4. Numerical Results

In this section, we give two specific numerical results to verify the previous theoretical analysis by comparing the exact solution with the numerical solution. We carry out numerical experiments by using the MATLAB 2017a with PC of AMD Ryzen 5 3500 U and 8 GB memory. And the L^1-error and the discrete L^2-error are measured with the following formulas, respectively, which are used to measure the numerical errors:

$$L^1 - \text{Error} = \max_{1\le n\le N}\left|u^n - U^n\right|, L^2 - \text{Error} = \max_{1\le n\le N}\left\|u^n - U^n\right\|. \tag{38}$$

For L^1-Error and L^2-error, we denote the convergence order by

$$L^i - \text{Rate} = \frac{\log\left(E_1/E_2\right)}{\log\left(h_1/h_2\right)}, \tag{39}$$

where $i = 1, 2$, E_1 and E_2 are errors that correspond to mesh sizes h_1 and h_2, respectively.

Table 1: Example 1: errors, temporal convergence rates, and CPU times with $\alpha = 0.2$.

M	N	L^2-error	L^2-rate	CPU time (s)
200	10	6.5323×10^{-4}	—	0.0607
200	20	1.6337×10^{-4}	2.00	0.0655
200	40	4.0872×10^{-5}	2.00	0.1023
200	80	1.0245×10^{-5}	2.00	0.2729
200	160	2.5885×10^{-6}	1.98	0.6354

Table 2: Example 1: errors, temporal convergence rates, and CPU times with $\alpha = 0.4$.

M	N	L^2-error	L^2-rate	CPU time (s)
200	10	2.0070×10^{-3}	—	0.0608
200	20	5.0208×10^{-4}	2.00	0.0735
200	40	1.2556×10^{-4}	2.00	0.1263
200	80	3.1419×10^{-5}	2.00	0.2742
200	160	7.8114×10^{-6}	2.00	0.6677

Table 3: Example 1: errors, temporal convergence rates, and CPU times with $\alpha = 0.6$.

M	N	L^2-error	L^2-rate	CPU time (s)
200	10	5.2707×10^{-3}	—	0.0434
200	20	1.3195×10^{-3}	2.00	0.0688
200	40	3.3002×10^{-4}	2.00	0.1136
200	80	8.2538×10^{-5}	2.00	0.3027
200	160	$2, 0661 \times 10^{-5}$	2.00	0.8396

Table 4: Example 1: errors, temporal convergence rates, and CPU times with $\alpha = 0.8$.

M	N	L^2-error	L^2-rate	CPU time (s)
200	10	1.6360×10^{-2}	—	0.0563
200	20	4.1088×10^{-3}	1.99	0.0758
200	40	1.0284×10^{-3}	2.00	0.1055
200	80	2.5720×10^{-4}	2.00	0.3392
200	160	6.4329×10^{-5}	2.00	0.8625

Table 5: Example 1: errors, spatial convergence rates, and CPU times with $\alpha = 0.3$.

M	N	L^2-error	L^2-rate	CPU time (s)
5	25	1.5507×10^{-2}	—	0.0241
10	100	1.3074×10^{-3}	3.57	0.0507
20	400	1.1421×10^{-4}	3.52	0.2967
40	1600	1.0066×10^{-5}	3.50	8.0681
80	6400	8.8903×10^{-7}	3.50	326.1065

Table 6: Example 1: errors, spatial convergence rates, and CPU times with $\alpha = 0.5$.

M	N	L^2-error	L^2-rate	CPU time (s)
5	25	1.5151×10^{-2}	—	0.0249
10	100	1.2779×10^{-3}	3.57	0.0412
20	400	1.1164×10^{-4}	3.52	0.3887
40	1600	9.8388×10^{-6}	3.50	8.1066
80	6400	8.6900×10^{-7}	3.50	223.9756

Example 1. We consider the equation (1) with $u(x,t) = t^3 \sin(\pi x)$ and a = 1.

$$\begin{cases} {}_0^{CF}D_t^{\alpha} u(x,t) = \dfrac{\partial^2 u}{\partial x^2} + f(x,t), & x \in [0,2], t \in [0,1], \\ u(x,0) = 0, & x \in [0,2], \\ u(0,t) = 0, u(2,t) = 0, & t \in [0,1], \end{cases} \tag{40}$$

where the source term $f(x,t) = \sin(\pi x)(3/(1-\alpha))\left((t^2/\sigma) - (2t/\sigma^2) + (2/\sigma^3)(1-e^{-\sigma t})\right) + \pi^2 t^3 \sin(\pi x)$ and $\sigma = \alpha/(1-\alpha)$.

We use the proposed scheme equation (11) to solve this example. First step, we tested the accuracy of the scheme in the direction of time. Taking the sufficiently dense spatial observation $M = 200$. In Tables 1–4, the convergence rates

Table 7: Example 1: errors, spatial convergence rates, and CPU times with $\alpha = 0.7$.

M	N	L^2-error	L^2-rate	CPU time (s)
5	25	1.4708×10^{-2}	—	0.0239
10	100	1.2414×10^{-3}	3.57	0.0437
20	400	1.0846×10^{-4}	3.52	0.3221
40	1600	9.5590×10^{-6}	3.50	8.2159
80	6400	8.4430×10^{-7}	3.50	232.8713

Table 8: Example 1: errors, spacial convergence rates, and CPU times with $\alpha = 0.9$.

M	N	L^2-error	L^2-rate	CPU time(s)
5	25	1.4643×10^{-2}	—	0.0252
10	100	1.2387×10^{-3}	3.56	0.0407
20	400	1.0846×10^{-4}	3.52	0.3341
40	1600	9.5460×10^{-6}	3.50	8.1655
80	6400	8.4318×10^{-7}	3.50	336.3633

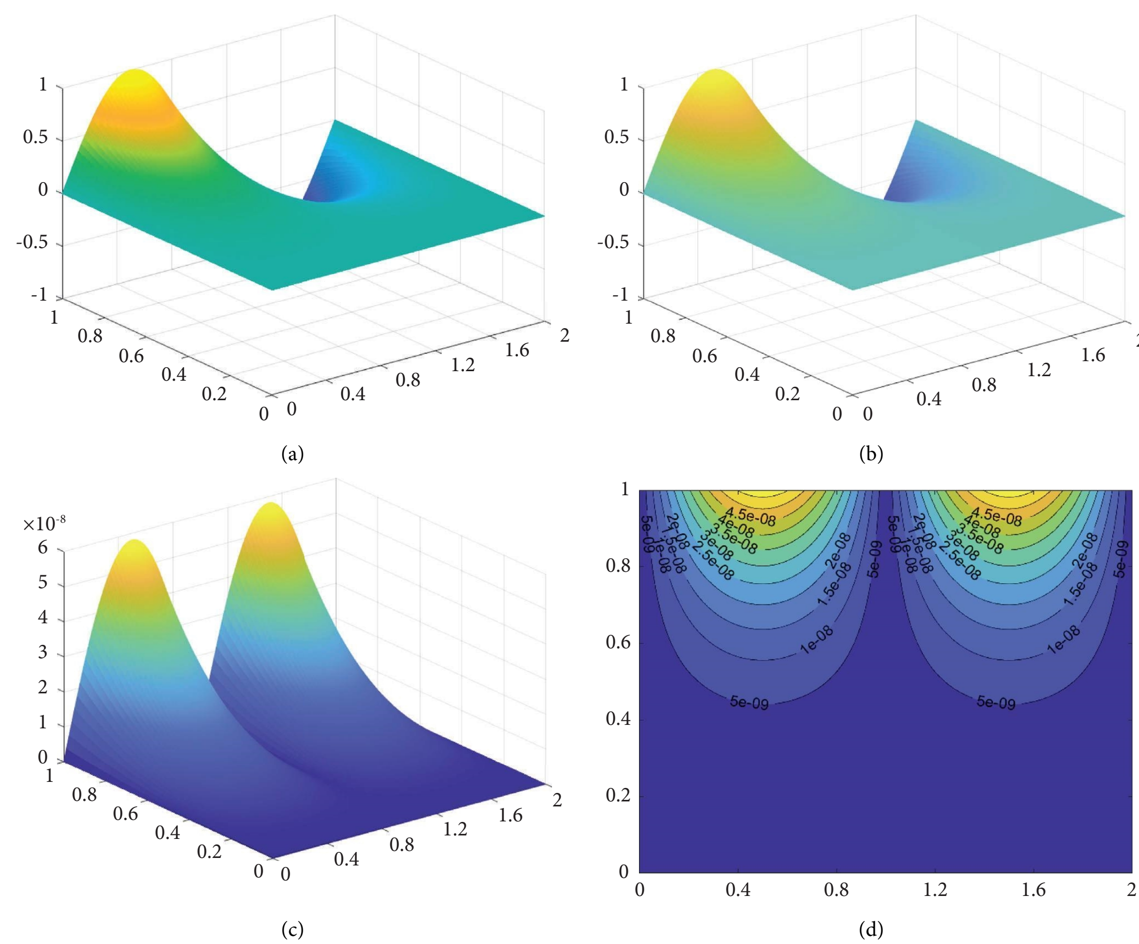

Figure 1: Example 1 with $\alpha = 0.25$ at $M = 100$ and $N = 5000$: (a) exact solution; (b) numerical solution; (c) absolute error; (d) contour plot of error.

for time are obtained as $O(\tau^2)$. And the errors, temporal convergence rates, and CPU times in the L^2-norm for different α (here $\alpha = 0.2, 0.4, 0.6, 0.8$) are shown in Tables 1–4. Experimental results show that the scheme produces a time approximation order close to 2. Second step, we tested the accuracy of the scheme in the direction of space with this example. In Tables 5–8, the convergence rates for space are obtained as $O(h^4)$. The spatial observation M and temporal observation N are chosen such that $N = M^2$ and $\alpha = 0.3, 0.5, 0.7, 0.9$. The errors, spacial convergence rates, and CPU times are shown in Tables 5–8, respectively. These conclusions are consistent with our analysis in Section 3.

In Figures 1 and 2, we show the exact solution, numerical solution, absolute error, and contour plot of error when $\alpha =$

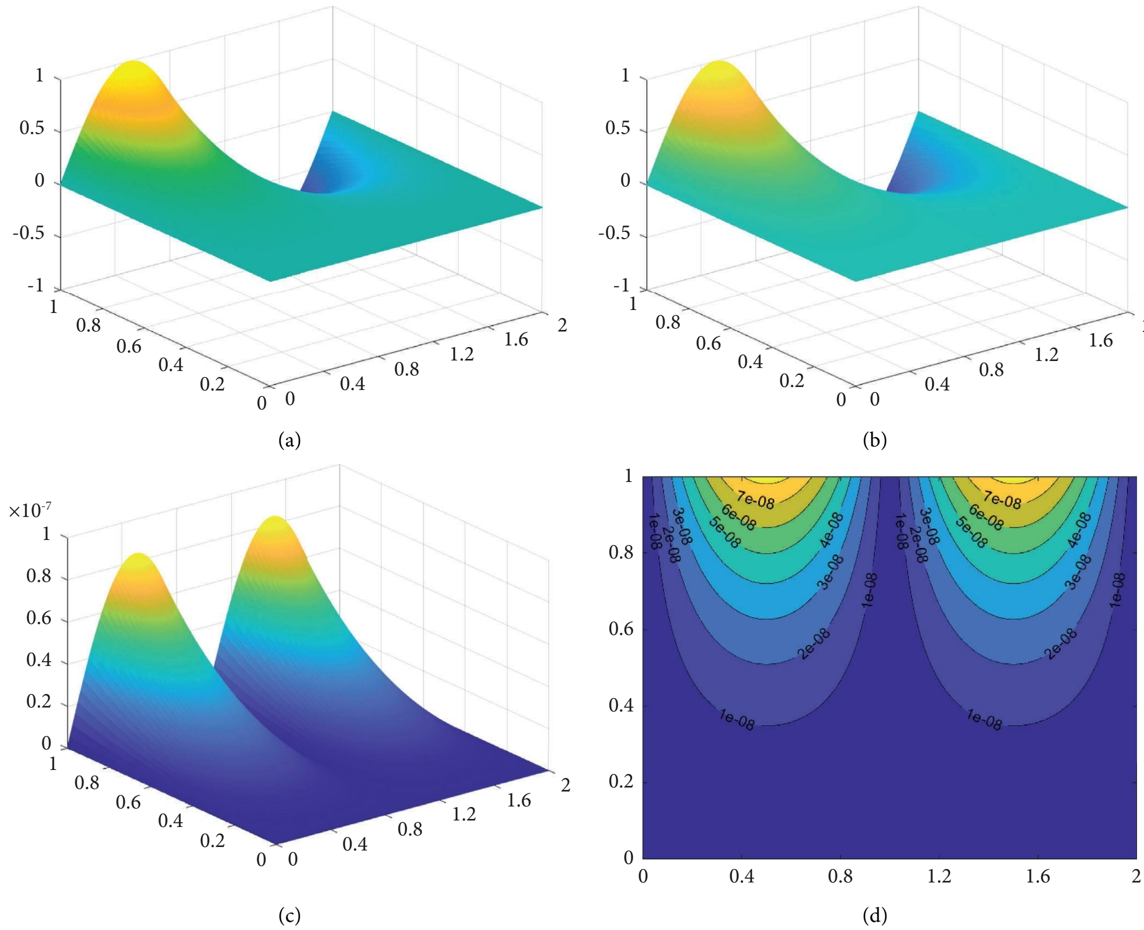

FIGURE 2: Example 1 with $\alpha = 0.95$ at $M = 100$ and $N = 5000$: (a) exact solution; (b) numerical solution; (c) absolute error; (d) contour plot of error.

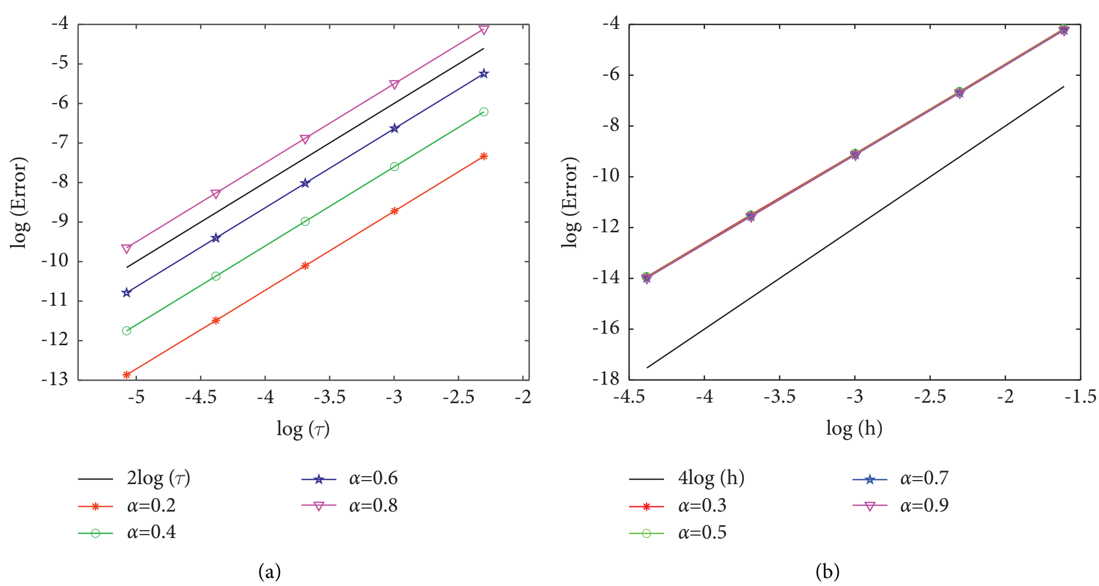

FIGURE 3: Example 1: $\log(Error)$ as a function of $\log(\tau)$ and $\log(h)$, respectively, for given α: (a) $\alpha = 0.2, 0.4, 0.6, 0.8$; (b) $\alpha = 0.3, 0.5, 0.7, 0.9$.

Table 9: Example 2: errors and temporal convergence rates with $a = 2$ and $M = 50$.

N	$\alpha = 0.1$		$\alpha = 0.5$		$\alpha = 0.9$	
	L^1-error	L^1-rate	L^1-error	L^1-rate	L^1-error	L^1-rate
20	6.1572×10^{-4}	—	4.9340×10^{-3}	—	1.5722×10^{-1}	—
40	1.5220×10^{-4}	2.02	1.2336×10^{-3}	2.00	4.0063×10^{-2}	1.97
80	3.6578×10^{-5}	2.06	3.0709×10^{-4}	2.01	1.0062×10^{-2}	1.99
160	7.6896×10^{-6}	2.25	7.5370×10^{-5}	2.03	2.5171×10^{-3}	2.00

Table 10: Example 2: errors and temporal convergence rates with $a = 1$ and $M = 50$.

N	$\alpha = 0.1$		$\alpha = 0.5$		$\alpha = 0.9$	
	L^1-error	L^1-rate	L^1-error	L^1-rate	L^1-error	L^1-rate
80	7.1847×10^{-5}	—	5.7221×10^{-4}	—	1.6674×10^{-2}	—
120	3.0905×10^{-5}	2.08	2.5558×10^{-4}	2.01	7.4175×10^{-3}	2.00
160	1.6577×10^{-5}	2.17	1.4301×10^{-4}	2.02	4.1731×10^{-3}	2.00
200	9.9459×10^{-6}	2.29	9.0899×10^{-5}	2.03	2.6707×10^{-3}	2.00

Table 11: Errors and temporal convergence rates in [48] with $M = 20000$.

N	$\alpha = 0.1$		$\alpha = 0.5$		$\alpha = 0.9$	
	L^1-error	L^1-rate	L^1-error	L^1-rate	L^1-error	L^1-rate
10	7.21×10^{-5}	—	8.48×10^{-4}	—	1.03×10^{-2}	—
20	1.80×10^{-5}	2.00	2.12×10^{-4}	2.00	2.64×10^{-3}	1.97
40	4.51×10^{-6}	2.00	5.29×10^{-5}	2.00	6.61×10^{-4}	2.00
80	1.13×10^{-6}	2.00	1.32×10^{-5}	2.00	1.66×10^{-4}	2.00

0.25 and 0.95 at $M = 100$ and $N = 5000$, respectively. It demonstrates that the numerical solution of equation (11) does well with the exact solution. In Figure 3(a), we show the errors in L^2-norm attain second order of accuracy in temporal direction for $\alpha = 0.2, 0.4, 0.6, 0.8$, respectively. In Figure 3(b), we show the errors in L^2-norm attain fourth order of accuracy in spatial direction for $\alpha = 0.3, 0.5, 0.7, 0.9$, respectively.

Example 2. In the second example, we consider the equation (1) with $u(x,t) = \sin(4t)\sin(\pi x)$:

$$\begin{cases} {}_0^{CF}D_t^{\alpha} u(x,t) = a\dfrac{\partial^2 u}{\partial x^2} + f(x,t), & x \in [0,1], t \in [0,2], \\ u(x,0) = 0, & x \in [0,1], \\ u(0,t) = 0, u(1,t) = 0, & t \in [0,2], \end{cases} \tag{41}$$

where the forcing function is $f(x,t) = \sin(\pi x)(4/((1-\alpha)(\sigma^2 + 16)))(\sigma\cos(4t) + 4\sin(4t) - \sigma e^{-\sigma t}) + a\pi^2 \sin(4t) \sin(\pi x)$ and $\sigma = \alpha/(1-\alpha)$.

As $a = 2$, the numerical results of Example 2 are shown in Table 9. Table 9 shows the errors and temporal convergence rates for $\alpha = 0.1, 0.5, 0.9$. We can find that when the diffusion coefficient changes and the time interval increases, numerical results are still consistent with our theoretical analysis.

In this example, when we choose the same parameters as in [48], that are $a = 1$ and $T = 2$, the numerical results of our method are shown in Table 10. The results of [48] are shown in Table 11. In the example of [48], $M = 20000$ and $N = 10, 20, 40, 80$ are used (see Table 11). However, in our method (see Table 10), we just use $M = 50$ and $N = 80, 120, 160, 200$. By comparison, it is found that our calculation accuracy is slightly lower than that of [48]; however, it takes a shorter time. We can also find that our method has a better convergence order when the value of α is smaller (for instance, $\alpha = 0.1$; there will be superconvergence with the value of N becoming larger).

5. Conclusion

In this paper, we present a higher-order CDS for the TFDE of the C-F type, proving that the scheme is unconditionally stable with temporal second-order accuracy and spatial fourth-order accuracy. The innovation in this paper is to discrete the equation using the C-F fractional derivatives and the compact difference operator to further improve the accuracy. Two numerical examples are given to verify the accuracy of the new scheme; the results are consistent with theoretical analysis. In the following study, we aim to solve the high-dimensional TFDE and coupled nonlinear problems using the method of our paper.

Data Availability

No underlying data were collected or produced in this study.

Conflicts of Interest

The authors declare that they have no conflicts of interest.

Acknowledgments

This work was supported by Natural Science Foundation of Xinjiang Uygur Autonomous Region (no. 2022D01E13), NSFC (no. 11861068), and Scientic Research Foundation for Outstanding Young Teachers of Xinjiang Normal University (nos. XJNU202012 and XJNU202112).

References

[1] Y. Feng and J. Liu, "Anomalous diffusion equation using a new general fractional derivative within the Miller-Ross kernel," *Modern Physics Letters B*, vol. 34, pp. 183–214, 2020.

[2] J. A. M. Carrer, B. S. Solheid, J. Trevelyan, and M. Seaid, "A boundary element method formulation based on the Caputo derivative for the solution of the anomalous diffusion problem," *Engineering Analysis with Boundary Elements*, vol. 122, pp. 132–144, 2021.

[3] S. M. Guo, L. Q. Mei, Y. Li, and Y. F. Sun, "The improved fractional sub-equation method and its applications to the space-time fractional differential equations in fluid mechanics," *Physics Letters A*, vol. 376, no. 4, pp. 407–411, 2012.

[4] C. C. Liu and M. L. Jin, "Some properties of solutions of a fourth-order parabolic equation for image processing," *Bulletin of the Malaysian Mathematical Sciences Society*, vol. 43, no. 1, pp. 333–353, 2020.

[5] M. H. Heydari, A. Atangana, Z. Avazzadeh, and M. R. Mahmoudi, "An operational matrix method for nonlinear variable-order time fractional reaction-diffusion equation involving Mittag-Leffler kernel," *The European Physical Journal Plus*, vol. 135, no. 2, pp. 237–319, 2020.

[6] H. J. Haubold, A. M. Mathai, and R. K. Saxena, "Further solutions of fractional reaction-diffusion equations in terms of the H-function," *Journal of Computational and Applied Mathematics*, vol. 235, no. 5, pp. 1311–1316, 2011.

[7] G. Pagnini, "The M-Wright function as a generalization of the Gaussian density for fractional diffusion processes," *Fractional Calculus and Applied Analysis*, vol. 16, no. 2, pp. 436–453, 2013.

[8] Y. Zhao, C. Shen, M. Qu, W. P. Bu, and Y. F. Tang, "Finite element methods for fractional diffusion equations," *International Journal of Modeling Simulation and Scientific Computing*, vol. 11, no. 04, Article ID 2030001, 2020.

[9] J. F. Huang, Y. F. Tang, L. Vázquez, and J. F. Yang, "Two finite difference schemes for time fractional diffusion-wave equation," *Numerical Algorithms*, vol. 64, no. 4, pp. 707–720, 2013.

[10] H. K. Pang and H. W. Sun, "Fourth order finite difference schemes for time-space fractional sub-diffusion equations," *Computers & Mathematics with Applications*, vol. 71, no. 6, pp. 1287–1302, 2016.

[11] A. Bhardwaj and A. Kumar, "A meshless method for time fractional nonlinear mixed diffusion and diffusion-wave equation," *Applied Numerical Mathematics*, vol. 160, pp. 146–165, 2021.

[12] Y. Gu and H. G. Sun, "A meshless method for solving three-dimensional time fractional diffusion equation with variable-order derivatives," *Applied Mathematical Modelling*, vol. 78, pp. 539–549, 2020.

[13] M. Badr, A. Yazdani, and H. Jafari, "Stability of a finite volume element method for the time-fractional advection-diffusion equation," *Numerical Methods for Partial Differential Equations*, vol. 34, no. 5, pp. 1459–1471, 2018.

[14] M. Ran and C. Zhang, "New compact difference scheme for solving the fourth-order time fractional sub-diffusion equation of the distributed order," *Applied Numerical Mathematics*, vol. 129, pp. 58–70, 2018.

[15] G. H. Gao and Z. Z. Sun, "A compact finite difference scheme for the fractional sub-diffusion equations," *Journal of Computational Physics*, vol. 230, no. 3, pp. 586–595, 2011.

[16] H. P. Ye, F. W. Liu, and V. Anh, "Compact difference scheme for distributed-order time-fractional diffusion-wave equation on bounded domains," *Journal of Computational Physics*, vol. 298, pp. 652–660, 2015.

[17] P. Zhang and H. Pu, "A second-order compact difference scheme for the fourth-order fractional sub-diffusion equation," *Numerical Algorithms*, vol. 76, no. 2, pp. 573–598, 2017.

[18] B. Guo, X. Pu, and F. Huang, *Fractional Partial Differential Equations and Their Numerical Solutions*, World Scientific, Singapore, 2015.

[19] R. Hilfer, *Applications of Fractional Calculus in Physics*, World Scientific, Singapore, 2000.

[20] I. Podlubny, *Fractional Differential Equations*, Academic Press, San Diego, USA, 1999.

[21] Y. L. Li, F. W. Liu, I. W. Turner, and T. Li, "Time-fractional diffusion equation for signal smoothing," *Applied Mathematics and Computation*, vol. 326, pp. 108–116, 2018.

[22] Z. W. Fang, H. W. Sun, and H. Wang, "A fast method for variable-order Caputo fractional derivative with applications to time-fractional diffusion equations," *Computers & Mathematics with Applications*, vol. 80, no. 5, pp. 1443–1458, 2020.

[23] V. Mehandiratta and M. Mehra, "A difference scheme for the time-fractional diffusion equation on a metric star graph," *Applied Numerical Mathematics*, vol. 158, pp. 152–163, 2020.

[24] A. Jannelli, M. Ruggieri, and M. P. Speciale, "Numerical solutions of space-fractional advection-diffusion equations with nonlinear source term," *Applied Numerical Mathematics*, vol. 155, pp. 93–102, 2020.

[25] J. Liu, J. Zhang, and X. D. Zhang, "Semi-discretized numerical solution for time fractional convection-diffusion equation by RBF-FD," *Applied Mathematics Letters*, vol. 128, Article ID 107880, 2022.

[26] M. Caputo and M. Fabrizio, "A new definition of fractional derivative without singular kernel," *Progress in Fractional Differentiation and Applications*, vol. 1, pp. 73–85, 2015.

[27] J. Losada and J. J. Nieto, "Properties of a new fractional derivative without singular kernel," *Progress in Fractional Differentiation and Applications*, vol. 1, pp. 87–92, 2015.

[28] J. K. Shi and M. H. Chen, "A second-order accurate scheme for two-dimensional space fractional diffusion equations with time Caputo-Fabrizio fractional derivative," *Applied Numerical Mathematics*, vol. 151, pp. 246–262, 2020.

[29] J. J. Nieto, "Solution of a fractional logistic ordinary differential equation," *Applied Mathematics Letters*, vol. 123, Article ID 107568, 2022.

[30] A. Atangana and R. T. Alqahtani, "Numerical approximation of the space-time Caputo-Fabrizio fractional derivative and application to groundweter polution equation," *Advances in Difference Equations*, vol. 2016, Article ID 1, 13 pages, 2016.

[31] I. A. Mirza and D. Vieru, "Fundamental solutions to advection-diffusion equation with time-fractional Caputo-Fabrizio derivative," *Computers & Mathematics with Applications*, vol. 73, pp. 1–10, 2017.

[32] A. Atangana, "On the new fractional derivative and application to nonlinear Fishers reaction-diffusion equation," *Applied Mathematics and Computation*, vol. 273, pp. 948–956, 2016.

[33] Z. Soori and A. Aminataei, "Two new approximations to Caputo-Fabrizio fractional equation on non-uniform meshes

and its applications," *Iranian Journal of Numerical Analysis and Optimization*, vol. 11, pp. 365–383, 2021.

[34] A. Atangana and B. S. T. Alkahtani, "Extension of the resistance, inductance, capacitance electrical circuit to fractional derivative without singular kernel," *Advances in Mechanical Engineering*, vol. 7, no. 6, Article ID 1687814015591937, 2015.

[35] A. Atangana and J. J. Nieto, "Numerical solution for the model of RLC circuit via the fractional derivative without singular kernel," *Advances in Mechanical Engineering*, vol. 7, no. 10, Article ID 1687814015813758, 2015.

[36] S. Abbas, M. Benchohra, and J. J. Nieto, "Caputo-Fabrizio fractional differential equations with non instantaneous impulses," *Rendiconti del Circolo Matematico di Palermo Series 2*, vol. 71, no. 1, pp. 131–144, 2022.

[37] S. M. Aydogan, D. Baleanu, A. Mousalou, and S. Rezapour, "On approximate solutions for two higher-order Caputo-Fabrizio fractional integro-differential equations," *Advances in Difference Equations*, vol. 2017, pp. 1–11, 2017.

[38] J. D. Djida and A. Atangana, "More generalized groundwater model with space-time Caputo-Fabrizio fractional differentiation," *Numerical Methods for Partial Differential Equations*, vol. 33, no. 5, pp. 1616–1627, 2017.

[39] M. A. Firoozjaee, H. Jafari, A. Lia, and D. Baleanu, "Numerical approach of Fokker-Planck equation with Caputo-Fabrizio fractional derivative using Ritz approximation," *Journal of Computational and Applied Mathematics*, vol. 339, pp. 367–373, 2018.

[40] E. F. Doungmo Goufo, "Application of the Caputo-Fabrizio fractional derivative without singular kernel to Korteweg-de Vries-Burgers equation," *Mathematical Modelling and Analysis*, vol. 21, no. 2, pp. 188–198, 2016.

[41] Z. G. Liu, A. J. Cheng, and X. L. Li, "A second order Crank-Nicolson scheme for fractional Cattaneo equation based on new fractional derivative," *Applied Mathematics and Computation*, vol. 311, pp. 361–374, 2017.

[42] J. R. Loh, A. Isah, C. Phang, and Y. T. Toh, "On the new properties of Caputo-Fabrizio operator and its application in deriving shifted Legendre operational matrix," *Applied Numerical Mathematics*, vol. 132, pp. 138–153, 2018.

[43] K. M. Owolabi and A. Atangana, "Analysis and application of new fractional Adams-Bashforth scheme with Caputo-Fabrizio derivative," *Chaos, Solitons & Fractals*, vol. 105, pp. 111–119, 2017.

[44] K. M. Owolabi and A. Atangana, "Numerical approximation of nonlinear fractional parabolic differential equations with Caputo-Fabrizio derivative in Riemann-Liouville sense," *Chaos, Solitons & Fractals*, vol. 99, pp. 171–179, 2017.

[45] R. Gorenflo, F. Mainardi, D. Moretti, and P. Paradisi, "Time fractional diffusion: a discrete random walk approach," *Nonlinear Dynamics*, vol. 29, no. 1/4, pp. 129–143, 2002.

[46] R. R. Nigmatullin, "The realization of the generalized transfer equation in a medium with fractal geometry," *Physica Status Solidi*, vol. 133, no. 1, pp. 425–430, 1986.

[47] D. D. Hu and X. N. Cao, "A fourth-order compact ADI scheme for two-dimensional Riesz space fractional nonlinear reaction-diffusion equation," *International Journal of Computer Mathematics*, vol. 97, no. 9, pp. 1928–1948, 2020.

[48] T. Akman, B. Yıldız, and D. Baleanu, "New discretization of Caputo-Fabrizio derivative," *Computational and Applied Mathematics*, vol. 37, no. 3, pp. 3307–3333, 2018.